Carbohydrate Polymers 115 (2015) 170–176

Contents lists available at ScienceDirect

Carbohydrate Polymers

journal homepage: www.elsevier.com/locate/carbpol

Structure and properties of hydroxyapatite/hydroxyethyl cellulose acetate composite films

K. Azzaoui[a,*], E. Mejdoubi[a], A. Lamhamdi[a], S. Zaoui[a], M. Berrabah[a], A. Elidrissi[b], B. Hammouti[b], Moustafa M.G. Fouda[c,d,**], Salem S. Al-Deyab[c]

[a] L.C.S.M.A., Faculté des Sciences, Université Mohammed Premier, 60 000 Oujda, Morocco
[b] L.C.A.E-URAC18, Faculté des Sciences, Université Mohammed Premier, 60 000 Oujda, Morocco
[c] Petrochemical Research Chair, Department of Chemistry, College of Science, King Saud University, PO Box 2455, Riyadh 11451, Saudi Arabia
[d] Textile Research Division, National Research Center, Dokki, P.O. 12622, Giza 12522, Egypt

ARTICLE INFO

Article history:
Received 23 July 2014
Received in revised form 12 August 2014
Accepted 13 August 2014
Available online 3 September 2014

Keywords:
Composite
Hydroxyapatite
Hydroxyethyle cellulose acetate
Biomaterials

ABSTRACT

The main aim of this research work was to develop a new inorganic–organic film. Hydroxyapaptite (HAp) particles that represent the inorganic phase was mixed well with hydroxyethyl cellulose acetate (HECA), which representing the organic phase and then the inorganic–organic films were fabricated by evaporating of the solvent. The structure as well as the properties of the formed films were characterized using different analytical tools such as field emission scanning electron microscopy (FEG-SEM), thermo-gravimetric analysis (TGA), Fourier transform infra-red (FT-IR) spectroscopy. The obtained results revealed that, the HAp nanoparticles was well dispersed and well immobilized throughout the formed films. This can be attributed to the role of the nano- and micropores in the HECA substrate. In addition, a strong interaction occurred between HAp and HECA matrix. The results showed also good thermal stability and miscibility as well.

1. Introduction

Recently, most of composite substances made from organic and inorganic phases have been appealed much attention. It is noticed that, polymer–composite substances have been broadly used in biomedical applications (Abdel-Mohsen, Aly, Hrdina, & Montaser, 2012; Hassan, Abdel-Mohsen, & Elhadidy, 2014; Ramakrishna, Mayer, Wintermantel, & Leong, 2001). Natural polymers (Abdel-Mohsen et al., 2013; Abdel-Mohsen, Aly, Hrdina, & Montaser, 2012; Abdel-Mohsen, Aly, Hrdina, Montaser, & Hebeish, 2012; Abdel-Mohsen, Hrdina, et al., 2012; Abdel-Mohsen, Aly, Hrdina, & Montaser, 2012), such as cellulose, chitin (Abdel-Mohsen, Aly, Hrdina, & Montaser, 2012; Abdel-Mohsen, Aly, Hrdina, Montaser, & Hebeish, 2012; Abdel-Mohsen, Hrdina, et al., 2012; Abdel-Mohsen, Aly, Hrdina, & Montaser, 2012; Abdel-Mohsen et al., 2014; Fouda, El-Aassar, & Al-Deyab, 2013; Přichystalová et al., 2014), corn protein, starch (El-Hamshary, Fouda, Moydeen, & Al-Deyab, 2014; El-Rafie et al., 2011; Hebeish, El-Naggar, et al., 2011) and soy protein isolate (SPI) (Bhardwaj, Mohanty, Drzal, Pourboghrat, & Misra, 2006; Lu & Larock, 2007; Yan, Chen, & Bangal, 2007) have become significant as it is renewable, biocombatible, biodegradable and also non toxic (Cheung, Lau, Lu, & Hui, 2007; Juntaro et al., 2008; Ragauskas et al., 2006; Sgriccia, Hawley, & Misra, 2008; Svagan, Samir, & Berglund, 2008; Yang et al., 2009). Cellulose is considered one of the most abundant natural polymers (Abdel-Rahman, Abdel-Mohsen, Fouda, Al Deyab, & Mohamed, 2013; Fouda & Fahmy, 2011; Hashem, Elshakankery, El-Aziz, Fouda, & Fahmy, 2011; Hebeish et al., 2011a), which is renewable and biodegradable and biocompatible too (Granja et al., 2001). It has been established a list of language applications in several fields such as textile manufacturing (Abdel-Mohsen, Aly, Hrdina, & Montaser, 2012; Abdel-Mohsen, Aly, Hrdina, Montaser, & Hebeish, 2012; Abdel-Mohsen, Hrdina, et al., 2012; Abdel-Mohsen, Aly, Hrdina, & Montaser, 2012) and has been widely used in the biomedical field as tissue engineering because of their well biocompatibility, similar to the hard and soft tissues mechanical properties of materials (Miyamoto, Takahashi, Ito, Inagaki, & Noishiki, 1989; Risbud & Bhonde, 2001).

In order to improve the solubility of cellulose as well as its derivatives, chemical modification has been carried out; using proper chemical entities such as: introducing water-soluble units (El-Shafei, Fouda, Knittel, & Schollmeyer, 2008), hydrophilic parts,

* Corresponding author at: Laboratoire du Solide Mineral, Fac Sci, Univ Mohammed Premier, Oujda, Morocco. Tel.: +212 536500603; fax: +212 536500603.
** Corresponding author. Tel.: +966 560773127.
E-mail addresses: k.azzaoui@yahoo.com (K. Azzaoui), m.gaballa@yahoo.com, mmfoudah@ksu.edu.sa (M.M.G. Fouda).

http://dx.doi.org/10.1016/j.carbpol.2014.08.089
0144-8617/

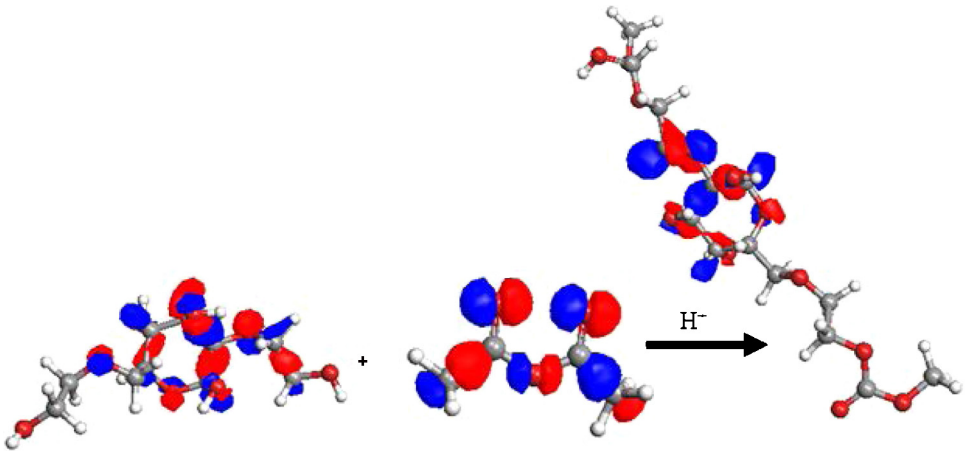

Fig. 1. Acylation reaction HEC.

in addition to bulky and hydrocarbon groups (Samaranayake & Glasser, 1993). Cellulose ether as well as hydroxyethyl cellulose (HEC) are frequently been applied into the industry due to their biocompatibility since they improve workability of the fresh material and their adherence to the substance too.

Hydroxyapaptite (HAp) in principal, is considered an inorganic component of natural bone (Azzaoui et al., 2014), and is mostly used in the field of tissue engineering because of its excellent biocompatibility, bioactivity, non-inflammatory, non-toxicity and osteoconductivity (Murugan & Ramakrishna, 2004). HAP has been utilized for the refining of proteins and plasmid DNA as resin, due to its double ion charged surface (such as Ca^{2+}, PO_4^{3-}), which can electrostatically drag the basic and acidic biomacromolecules, respectively (Schröder, Jönsson, & Poole, 2003).

Lately, the higher attraction of HAp towards protein has been utilized for binding and releasing the active biological molecules (Jongpaiboonkit, Franklin-Ford, & Murphy, 2009). It is noticed that the integration of HAp into poly (L-lactide) leads to an improvement in the protein adsorption capacity. This can be attributed to that; HAp has not only a high affinity to protein but also alter the scaffold surface morphology making them more appropriate for protein absorption (Wei & Ma, 2004). No doubt that, natural polymers are most likely, biocompatible and biodegradable, hence they are important for tissue engineering, as a result, the incorporation of n-HAp into the biopolymer matrix leads to an improvement in mechanical properties, in addition, incorporation of nanotopographic features can mimic the nanostructure of bone (Swetha et al., 2010).

In the present work, the synthesis of novel cellulose derivative (HECA) that is soluble in most organic solvents as DMF, starting from Hydroxyethyl cellulose (HEC) prepared from "Stipa Tenacissima" cellulose of Eastern Morocco and acetic anhydride (Elidrissi, El barkany, Amhamdi, & Maaroufi, 2013) has been described. The resulted product (HECA) will have the same characteristic properties that each biopolymer; cellulose acetate (CA) and hydroxyethyl cellulose (HEC) has. The resulted product (HECA) is mixed well at the same time with hydroxyapatite modified by PEG 1000 to give the corresponding membrane.

2. Materials and methods

2.1. Materials

Hydroxyethyl cellulose acetate (HECA) and hydroxyapatite (HAp) was synthesized in our laboratory. $Ca(NO_3)_2{\cdot}4H_2O$ (99%), $(NH_4)_2HPO_4$ (99%) and PEG 1000 were purchased from Aldrich, Germany. High purity distilled water was used throughout the whole experiments.

2.2. Hydroxyethyl cellulose acetylating

2 g of HEC (8.83 mmol) were subjected to drying at 40 °C for 24 h. The dried sample was kept in a three-necked flask. Different amounts of acetic anhydride were added respectively to the mixture 1 (8.83 mmol); 1.5, 2, 3, 6, 9, 12 and 15. The reaction time as well as the reaction temperature have been changed respectively between (15, 30, 45, 60 and 90 min) and (0, 25, 50, 60, 90 °C). The mixture was left under stirring for 15 min. Perchloric acid is added slowly at room temperature and the mixture is left again under stirring for complete homogenization. According to the solubility diagram, determined using HSP, water or diethyl ether was used as medium for the precipitation of the obtained product. The product was filtered using vacuum pump, followed by washing three times with cold water/cold ether and left for drying at 60 °C for 24 h and finally is kept in desiccator having P_2O_5 for one week. The resulted HECA was further purified using the dissolution–precipitation method in different solvents taking into account their DS according to the solubility stadium diagram, which already presented. The recovered product was characterized and evaluated using different analytical techniques (Fig. 1).

2.3. Synthesis of thin composite

Calcium nitrate tetra hydrate and di-ammonium hydrogen phosphate were used, as starting constituents reagents used in the preparation of hydroxyapatite. HAp was synthesized according to the modified wet chemical method described by Azzaoui et al., 2013. "At 25 °C, 11.76 g of Ca $(NO_3)_2$, $4H_2O$ was first dissolved in a 100 ml volume of water". "A solution of 4.06 g $(NH_4)_2HPO_4$ was dissolved in 100 ml volume of water and then added to the Ca $(NO_3)_2$, $4H_2O$ solution over a period of 30 min". "The amount of reagents in the solution was calculated to obtain a Ca/P molar ratio value

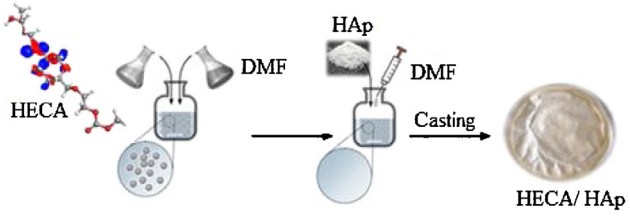

Fig. 2. Synthesis of membranes based on HECA/HAp/PEG 1000.

equals 1.67, corresponding to a stoichiometric Hap". "About of the polyethylene glycol was added along with the mixture". "The pH of the slurry was measured digitally during the precipitation reaction, reaching a final value of pH 10.5" (Azzaoui et al., 2013).

HECA polymer were dissolved in DMF at 40 °C under stirring in order to form solution named A. Hydroxyapatite (HAp) that dispersed in DMF at room temperature is considered as (Solution B), is further added to solution A. The colour of the resulted mixture is turned to opaque milky white after about 30 min. In addition, with temperature control to 40 °C and with a rate of 2 °C/min for almost 2 h, thin films were obtained, and then cleaned in absolute ethanol to remove any possible impurities in the formed film (Fig. 2).

3. Results and discussion

Using FTIR analysis, the interaction between inorganic and organic constituents has been extensively studied. Fig. 3 displays the FTIR spectra of unmodified HEC (1) and hydroxyethyl cellulose acetate samples (HECA) with different degree of substitution (DS = 2.4). As soon as the acetylation reaction between acetic anhydride and HEC takes place, the alteration may be verified by the carbonyl ester band at 1739 cm^{-1} and the broad band intensity of the OH groups, assigned to alcohol, decrease to 3480 cm^{-1}. The peaks located at ~2948 cm^{-1} and ~2885 cm^{-1} are attributed to ν(C—H) and ν(C—H_2) groups respectively (Garside & Wyeth, 2003). The band positioned also at 1647 cm^{-1} relates to the bending mode of the naturally absorbed water (Pastorova, Botto, Arisz, & Boon, 1994). The absorbance at 1375 cm^{-1} arises from the C—CH_3 vibration, moreover the peak at 1242 cm^{-1} is originated from $\nu(C—O)_{ester}$ vibration. However, the bands allocated to the hydroxyl ion of hydroxyapatite are found at 3572 cm^{-1} and 630 cm^{-1}. The bands allocated to groups of PO_4^{3-} are observed at 1090 cm^{-1}, 1047 cm^{-1}, 962 cm^{-1}, 602 cm^{-1} and 572 cm^{-1}. We also observe the decrease in band intensity of the hydroxyl (OH^-)

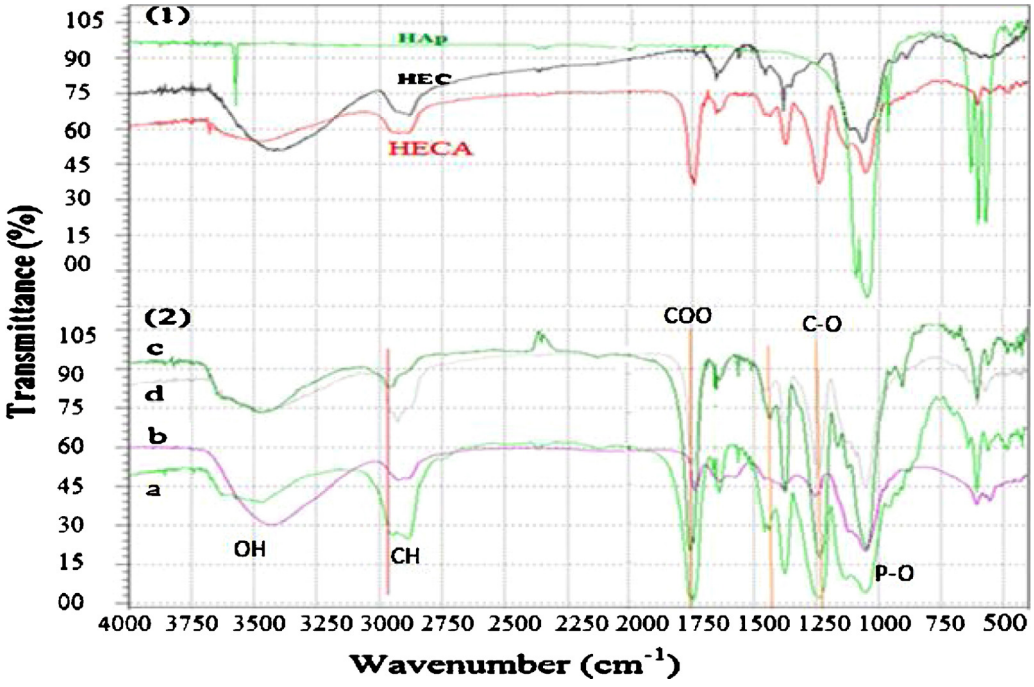

Fig. 3. Infrared absorption spectra of composite HECA/TETA/PEG 1000, with molar ratios respectively. *a* = 100/00, *b* = 10/80/10, *c* = 20/70/10 and *d* = 30/60/10.

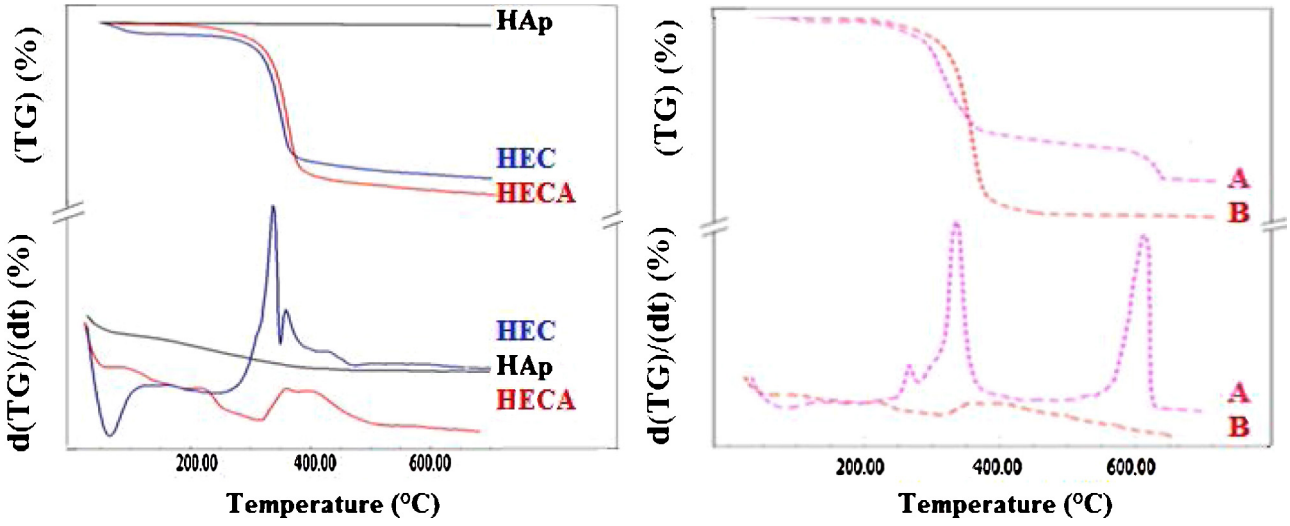

Fig. 4. TGA and DTA curves of HEC, and HECA HAp/HAp/PEG 1000 composite with molar ratios respectively. A = 10/80/10; B = 100/00.00.

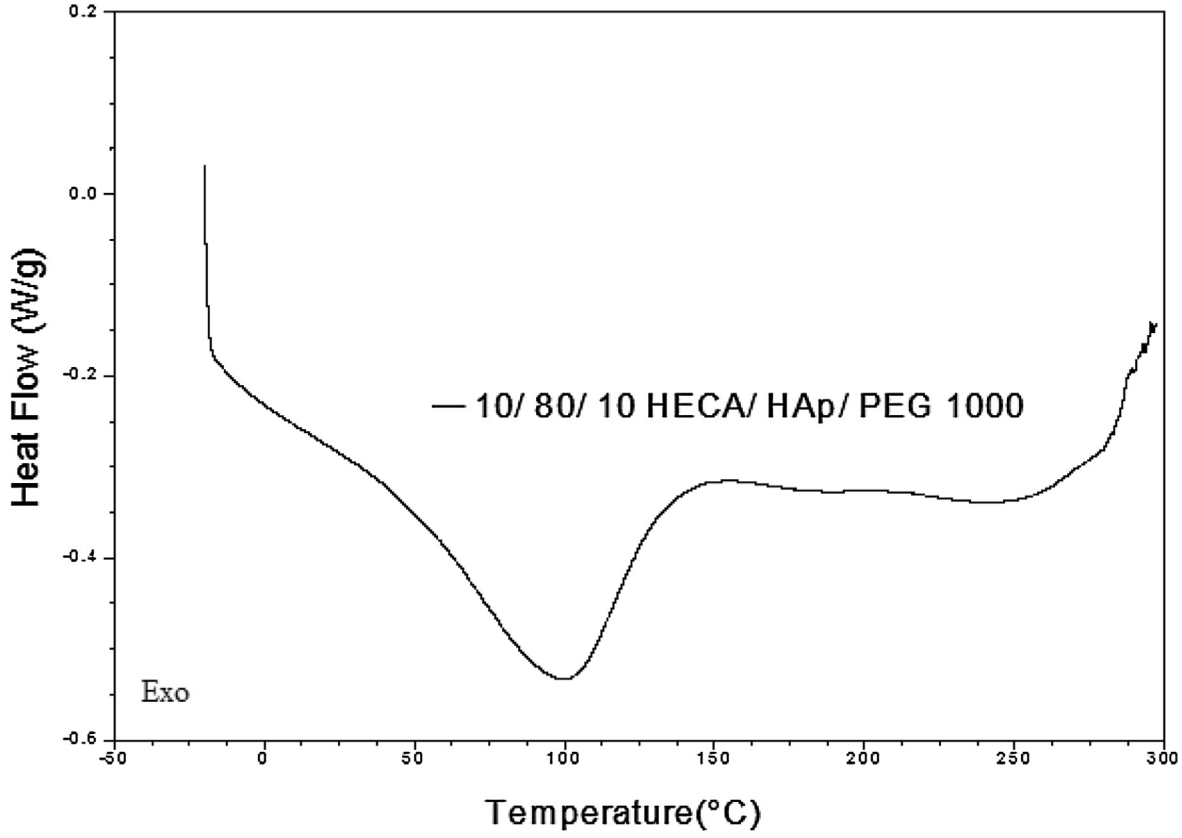

Fig. 5. DSC curves of HECA/HAp/PEG 1000 composite.

located and 3435 cm^{-1} 630 cm^{-1} of the IR spectra of the grafted materials when the level of grafting increases. We also note the change in the intensity of the bands at 2879–2849 cm^{-1} for composite A, due to vibrations ν(CH) and ν(C—H_2) groups, respectively (Liu, Sun, Zhang, Ren, & Geng, 2006), and a displacement of the 2879–2950, 2925–2955 and 2943–2960 cm^{-1} for the composites B, C and D, respectively. Other vibration bands were observed around 1638 cm^{-1} corresponds to the bending mode of water absorbed naturally (Zhou, Zhang, Li, Wu, & Cheng, 2005). The absorbance at 1373 cm^{-1} is derived from the vibration-CH_3 (spectrum A), and a movement thereof to 1376, 1379 and 1384 cm^{-1}. The peak at 1239 cm^{-1} is originated ν(CO) Vibration (spectrum A) ester, and a movement thereof to 1236, 1240 and 1253 cm^{-1}.

Table 1
Results and conditions of the HEC acetylation.

Spl	T (min)	T (°C)	Eq. nb.[b]	DS. IR-TF	DS ^{1}H HMR	Solvent			
						EtOH	THF	DMSO	H_2O
1	60	60	1	0.41	–	O	x	O	x
2	60	60	1, 5	0.57	–	O	x	O	x
3	60	60	2	0.7	0.72	O	x	O	x
4	60	60	3	1.07	1.27	O	x	O	x
5	60	60	6	1.4	–	O	O	O	x
6	60	60	9	1.61	–	O	O	O	x
7	60	60	12	2.24	2.4	x	O	O	x
8	60	60	15	2.6[c]	–	x	O	O	
9	15	25	6	0.26	–	x	x	O	O
10	30	25	6	0.34	–	O	x	O	O
11	60	60	6	0.45	–	O	x	O	x
12	90	60	6	0.6	–	O	x	O	x
13	60	25	6	0.81	–	O	x	O	x
14	60	0	6	0.35	–	O	x	O	O
15	60	25	6	0.6	–	O	x	O	x
16	60	50	6	1.14	–	O	x	O	x
17	60	60	6	1.4	–	O	O	O	x
18	60	85	6	3.2	–	O	O	O	x
S.c[a]	60	25	6	0.26	–	O	x	O	O

x, non soluble; O, soluble.
[a] Acetylation without catalyst.
[b] 1 eq amount to acetyl one hydroxyl group.
[c] Determined by volumetric method (ref).

3.1. Thermal study

TGA diagrams show/display that composites have two stages of weight loss: the first is recorded between 25 and 160° C corresponds to desorption of water adsorbed on the surface of the apatite and light little organic matter related to apatitic matrix. The second stage of HEC decompose between 266–356 °C and 280–375 °C for HECA. While HECA/HAp/PEG 1000 have three mass loss: the first between 25 and 100 °C, the second between 269 and 353 °C, and the third between 581 and 624 °C, respectively. This increase in the decomposition temperature suggested that the thermal stability of HECA is more important than that of HEC, and the thermal stability of HECA/HAp/PEG 1000 composite is higher than that of HECA. Similar results were also observed in the case of acetates cellulose (Liu et al., 2006). The TGA and DTG curves of the films were shown in Fig. 4. Noticeably, the thermal stability of all films increased with loading of HAp nanoparticles. Results designated further the strong interaction occurred between the cellulose and HAp.

3.2. Characterization by DSC

Fig. 5 shows different thermal occurrences (detected by differential scanning calorimetry) that occur on/composite HECA/HAp/PEG 1000. The glass transition around 99 °C and a melting temperature of the composite around the order of 256 °C. It is well documented in the literature that in the case of HECA, the principle endothermic peak is mostly due to the depolymerization of HEC, while the heat is due to the formation of CO_2. Each thermal transition will be discussed in the following paragraphs.

3.3. Morphology of HECA/HAp/PEG 1000 composite

The observation of particle composites based HECA/HAp/PEG 1000 by microscopic SEM-FEG can appreciate the size, shape, distribution and microstructure of granules. Fig. 6 shows FEG-SEM observation images of treated hydroxyapatite particles. It may be noted that the size distribution of about 92 nm. The composite

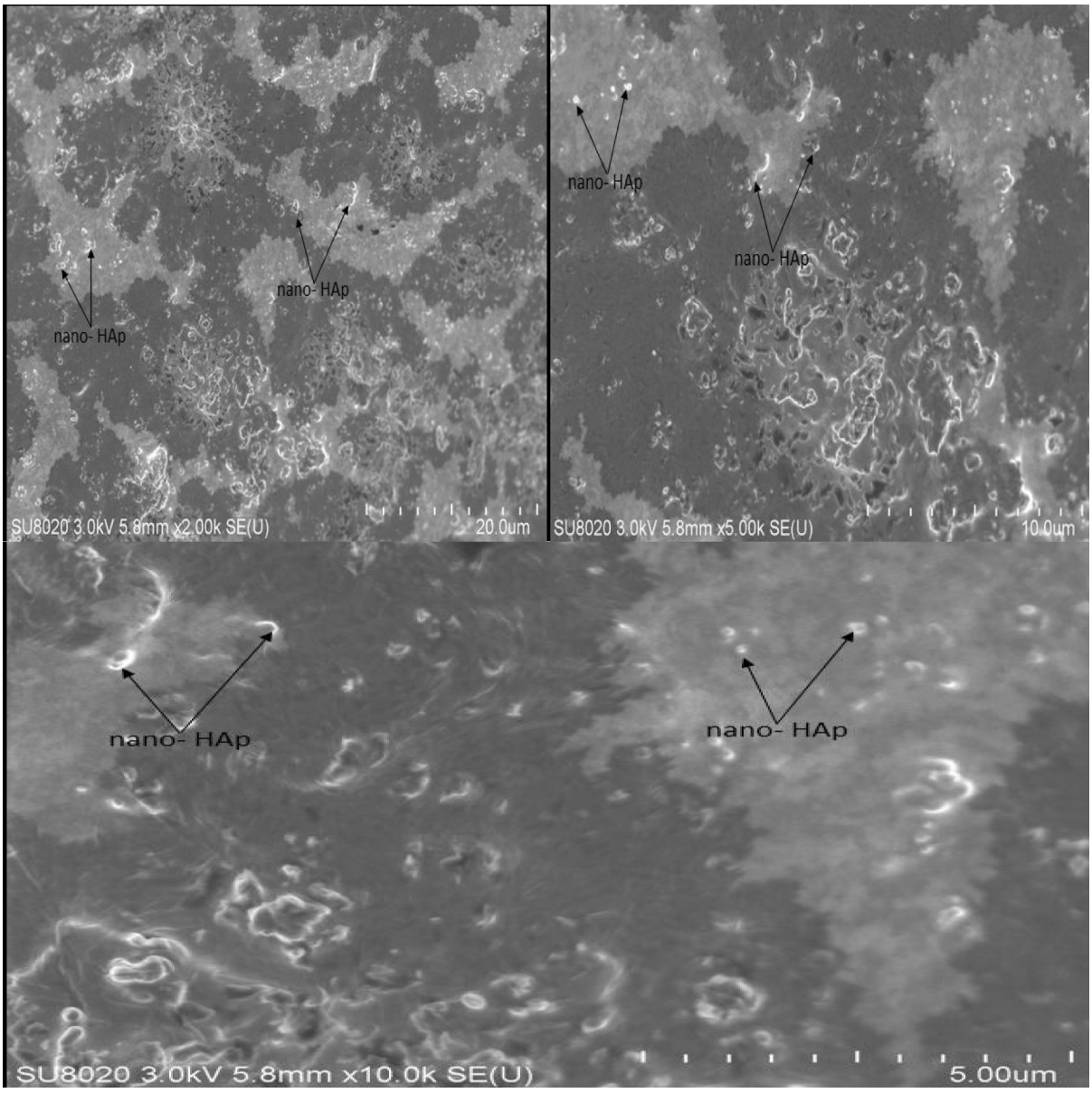

Fig. 6. SEM-FEG composite HECA/HAp_t/PEG 1000 composite with molar ratio. A = 10/80/10.

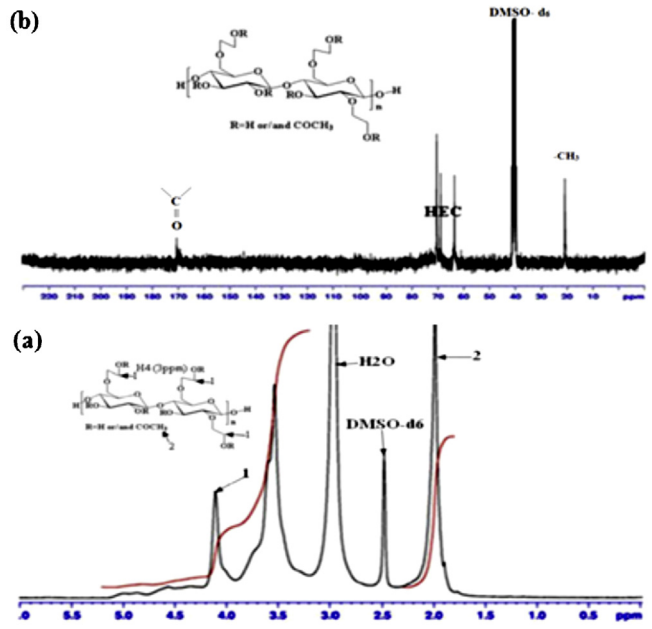

Fig. 7. ^{1}H NMR Spectra of HECA DS = 2.4 (a) and ^{13}C NMR Spectra of HECA DS = 2.4(b).

nanoparticles is visible to show that these nanoparticles are highly granular and composed of crystals of small size gives it its properties bioactivity.

3.4. NMR study

Initially, all samples must be purified. The represented spectra, Fig. 7(a) displays the peak ascribed to the water at ~3 ppm. The methylene proton of HEC was between ~3.5 ppm and ~3.6 ppm and were overlapped with the broad ring proton signals (2.8–5.6 ppm) of cellulose. The synthesis of HECA was successfully evidenced by the existing of a new signals at 2.0 ppm and at 4.11 ppm which are ascribed respectively to the acetyl protons and to the methylene in α of the ester. The HECA DS values were also predictable using ^{1}H NMR technique from the acetyl protons to the total HEC proton integrations as declared above and the results are shortened in Table 1.

Fig. 7(b) depicts the carbon ring of HECA with DS = 2.4, in DMSO-d_6 at 360 K. The signals at 21 ppm and ~170 ppm in the ^{13}C NMR spectra designate the presence of the carbon of acetyl group and the carbonyl ester respectively. The assignments of the other peaks are, according to Qi Zhou et al. (Zhou et al., 2005) and Juli et al. (Li, Xie, Cheng, Nickol, & Wang, 1999), ascribed to the HEC carbon region (60–105 ppm).

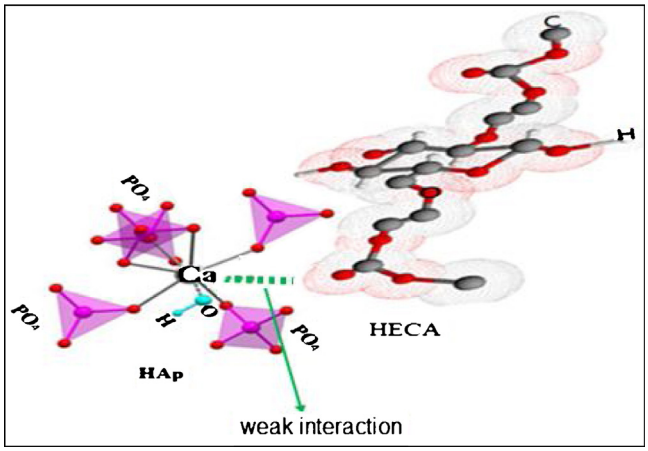

Fig. 8. Schematic model of the weak interaction between the CO groups in HECA and the HAp_t.

Based on the above results, a schematic model of hydrogen bonding between CO groups in HECA and the surface of OH groups in HAp nanoparticles was considered as revealed in Fig. 8. The molecular chains of HECA polymer are randomly twisting and inhibit reversible phase from irreversible strain that hang on the physical twisting during inter-transition from glassy state to rubbery state. Nevertheless, in the nanocomposites the interpenetrating networks were designed due to a physical crosslinking by the weak interaction, which worked as a stationary phase during the recovery of memory shape, as shown in Fig. 8. The model may also be used to describe the above results (e.g., the outcome from FTIR, TGA/TDA and DSC).

4. Conclusion

Grafting the HAp was successfully incorporated into the matrix HECA. The porous structure of the composite, HECA/HAp/PEG 1000 has been playing an important role in the stabilization and dispersion of TETA particles due to the interaction of strong intermolecular hydrogen bonding between HECA and HAp. Particles HAp were uniformly dispersed and immobilized in inorganic–organic composites. The analysis by FTIR spectroscopy showed the presence of specific interaction between HECA and HAp in mixtures HECA/HAp/PEG 1000. In addition, the film morphology observed by FEG-SEM microscopy shows that mixtures HECA/HAp/PEG 1000 are more homogeneous and particles HECA incorporated into the matrix of HAp are thinner.

Acknowledgment

The authors extend their appreciation to the Deanship of Scientific Research at king Saud University for funding the work through the research group project no. RGP-No. 089.

References

Abdel-Mohsen, A. M., Abdel-Rahman, R. M., Fouda, M. M. G., Vojtova, L., Uhrova, L., Hassan, A. F., et al. (2014). Preparation, characterization and cytotoxicity of schizophyllan/silver nanoparticle composite. *Carbohydrate Polymers*, *102*(1), 238–245.

Abdel-Mohsen, A. M., Aly, A. S., & Hrdina, R. (2012). A novel method for the preparation of silver/chitosan-O-methoxy polyethylene glycol core shell nanoparticles. *Journal of Polymers and Environment*, *20*, 459–468.

Abdel-Mohsen, A. M., Aly, A. S., Hrdina, R., Montaser, A. S., & Hebeish, A. (2012). Biomedical textiles through multifunctioalization of cotton fabrics using innovative methoxypolyethylene glycol-N-chitosan graft copolymer. *Journal of Polymers and the Environment*, *20*(1), 104–116.

Abdel-Mohsen, A. M., Hrdina, R., Burgert, L., Abdel-Rahman, R. M., Hašová, M., Šmejkalová, D., et al. (2013). Antibacterial activity and cell viability of hyaluronan fiber with silver nanoparticles. *Carbohydrate Polymers*, *92*(2), 1177–1187.

Abdel-Mohsen, A. M., Hrdina, R., Burgert, L., Krylová, G., Abdel-Rahman, R. M., Krejčová, A., et al. (2012). Green synthesis of hyaluronan fibers with silver nanoparticles. *Carbohydrate Polymers*, *89*(2), 411–422.

Abdel-Mohsen, M. A., Aly, A. S., Hrdina, R., & Montaser, A. S. (2012). Eco-synthesis of PVA/chitosan hydrogels for biomedical application. *Journal of Polymers and Environment*, *19*, 1005–1012.

Abdel-Rahman, R. M., Abdel-Mohsen, A. M., Fouda, M. M. G., Al Deyab, S. S., & Mohamed, A. S. (2013). Finishing of cellulosic fabrics with chitosan/polyethylene glycol-siloxane to improve their performance and antibacterial properties. *Life Science Journal*, *10*(4), 834–839.

Azzaoui, K., Lamhamdi, A., Mejdoubi, E., Berrabah, M., ELidrissi, A., Hammouti, B., et al. (2013). Synthesis of nanostructured hydroxyapatite in presence of polyethylene glycol 1000. *Journal of Chemical and Pharmaceutical Research*, *5*(12), 1209–1216.

Azzaoui, K., Lamhamdi, A., Mejdoubi, E. M., Berrabah, M., Hammouti, B., Elidrissi, A., et al. (2014). Synthesis and characterization of composite based on cellulose acetate and hydroxyapatite application to the absorption of harmful substances. *Carbohydrate Polymers*, *111*(0), 41–46.

Bhardwaj, R., Mohanty, A. K., Drzal, L. T., Pourboghrat, F., & Misra, M. (2006). Renewable resource-based green composites from recycled cellulose fiber and

poly(3-hydroxybutyrate-co-3-hydroxyvalerate) bioplastic. *Biomacromolecules*, *7*(6), 2044–2051.
Cheung, H.-Y., Lau, K.-T., Lu, T.-P., & Hui, D. (2007). A critical review on polymer-based bio-engineered materials for scaffold development. *Composites Part B: Engineering*, *38*(3), 291–300.
El-Hamshary, H., Fouda, M. M. G., Moydeen, M., & Al-Deyab, S. S. (2014). Removal of heavy metal using poly(N-vinylimidazole)-grafted-carboxymethylated starch. *International Journal of Biological Macromolecules*, *66*(0), 289–294.
El-Rafie, M. H., El-Naggar, M. E., Ramadan, M. A., Fouda, M. M. G., Al-Deyab, S. S., & Hebeish, A. (2011). Environmental synthesis of silver nanoparticles using hydroxypropyl starch and their characterization. *Carbohydrate Polymers*, *86*(2), 630–635.
El-Shafei, A. M., Fouda, M. M. G., Knittel, D., & Schollmeyer, E. (2008). Antibacterial activity of cationically modified cotton fabric with carboxymethyl chitosan. *Journal of Applied Polymer Science*, *110*(3), 1289–1296.
Elidrissi, A., El barkany, S., Amhamdi, H., & Maaroufi, A.-K. (2013). Synthesis and characterization of the new cellulose derivative films based on the hydroxyethyl cellulose prepared from esparto stipa tenacissima cellulose of Eastern Morocco. II. Esterification with acyl chlorides in a homogeneous medium. *Journal of Applied Polymer Science*, *127*(5), 3633–3644.
Fouda, M. M. G., El-Aassar, M. R., & Al-Deyab, S. S. (2013). Antimicrobial activity of carboxymethyl chitosan/polyethylene oxide nanofibers embedded silver nanoparticles. *Carbohydrate Polymers*, *92*(2), 1012–1017.
Fouda, M. M. G., & Fahmy, H. M. (2011). Multifunctional finish and cotton cellulose fabric. *Carbohydrate Polymers*, *86*(2), 625–629.
Garside, P., & Wyeth, P. (2003). Identification of cellulosic fibres by FTIR Spectroscopy – Thread and single fibre analysis by attenuated total reflectance. *Studies in Conservation*, *48*(4), 269–275.
Granja, P. L., Barbosa, M. A., Pouységu, L., De Jéso, B., Rouais, F., & Baquey, C. (2001). Cellulose phosphates as biomaterials. Mineralization of chemically modified regenerated cellulose hydrogels. *Journal of Materials Science*, *36*(9), 2163–2172.
Hashem, M., Elshakankery, M. H., El-Aziz, S. M. A., Fouda, M. M. G., & Fahmy, H. M. (2011). Improving easy care properties of cotton fabric via dual effect of ester and ionic crosslinking. *Carbohydrate Polymers*, *86*(4), 1692–1698.
Hassan, A. F., Abdel-Mohsen, A. M., & Elhadidy, H. (2014). Adsorption of arsenic by activated carbon, calcium alginate and their composite beads. *International Journal of Biological Macromolecules*, *68*(0), 125–130.
Hebeish, A., Abdel-Mohdy, F. A., Fouda, M. M. G., Elsaid, Z., Essam, S., Tammam, G. H., et al. (2011). Green synthesis of easy care and antimicrobial cotton fabrics. *Carbohydrate Polymers*, *86*(4), 1684–1691.
Hebeish, A., El-Naggar, M. E., Fouda, M. M. G., Ramadan, M. A., Al-Deyab, S. S., & El-Rafie, M. H. (2011). Highly effective antibacterial textiles containing green synthesized silver nanoparticles. *Carbohydrate Polymers*, *86*(2), 936–940.
Jongpaiboonkit, L., Franklin-Ford, T., & Murphy, W. L. (2009). Growth of hydroxyapatite coatings on biodegradable polymer microspheres. *ACS Applied Materials & Interfaces*, *1*(7), 1504–1511.
Juntaro, J., Pommet, M., Kalinka, G., Mantalaris, A., Shaffer, M. S. P., & Bismarck, A. (2008). Creating hierarchical structures in renewable composites by attaching bacterial cellulose onto sisal fibers. *Advanced Materials*, *20*(16), 3122–3126.
Li, J., Xie, W., Cheng, H. N., Nickol, R. G., & Wang, P. G. (1999). Polycaprolactone-modified hydroxyethylcellulose films prepared by lipase-catalyzed ring-opening polymerization. *Macromolecules*, *32*(8), 2789–2792.
Liu, C. F., Sun, R. C., Zhang, A. P., Ren, J. L., & Geng, Z. C. (2006). Structural and thermal characterization of sugarcane bagasse cellulose succinates prepared in ionic liquid. *Polymer Degradation and Stability*, *91*(12), 3040–3047.
Lu, Y., & Larock, R. C. (2007). Fabrication, morphology and properties of soybean oil-based composites reinforced with continuous glass fibers. *Macromolecular Materials and Engineering*, *292*(10–11), 1085–1094.
Miyamoto, T., Takahashi, S.-i., Ito, H., Inagaki, H., & Noishiki, Y. (1989). Tissue biocompatibility of cellulose and its derivatives. *Journal of Biomedical Materials Research*, *23*(1), 125–133.
Murugan, R., & Ramakrishna, S. (2004). Bioresorbable composite bone paste using polysaccharide based nano hydroxyapatite. *Biomaterials*, *25*(17), 3829–3835.
Pastorova, I., Botto, R. E., Arisz, P. W., & Boon, J. J. (1994). Cellulose char structure: a combined analytical Py-GC-MS, FTIR, and NMR study. *Carbohydrate Research*, *262*(1), 27–47.
Přichystalová, H., Almonasy, N., Abdel-Mohsen, A. M., Abdel-Rahman, R. M., Fouda, M. M. G., Vojtova, L., et al. (2014). Synthesis, characterization and antibacterial activity of new fluorescent chitosan derivatives. *International Journal of Biological Macromolecules*, *65*, 234–240.
Ragauskas, A. J., Williams, C. K., Davison, B. H., Britovsek, G., Cairney, J., Eckert, C. A., et al. (2006). The path forward for biofuels and biomaterials. *Science*, *311*(5760), 484–489.
Ramakrishna, S., Mayer, J., Wintermantel, E., & Leong, K. W. (2001). Biomedical applications of polymer–composite materials: A review. *Composites Science and Technology*, *61*(9), 1189–1224.
Risbud, M. V., & Bhonde, R. R. (2001). Suitability of cellulose molecular dialysis membrane for bioartificial pancreas: In vitro biocompatibility studies. *Journal of Biomedical Materials Research*, *54*(3), 436–444.
Samaranayake, G., & Glasser, W. G. (1993). Cellulose derivatives with low DS. I. A novel acylation system. *Carbohydrate Polymers*, *22*(1), 1–7.
Schröder, E., Jönsson, J., & Poole, T. L. (2003). Hydroxyapatite chromatography: Altering the phosphate-dependent elution profile of protein as a function of pH. *Analytical Biochemistry*, *313*(1), 176–178.
Sgriccia, N., Hawley, M. C., & Misra, M. (2008). Characterization of natural fiber surfaces and natural fiber composites. *Composites Part A: Applied Science and Manufacturing*, *39*(10), 1632–1637.
Svagan, A. J., Samir, M. A. S. A., & Berglund, L. A. (2008). Biomimetic foams of high mechanical performance based on nanostructured cell walls reinforced by native cellulose nanofibrils. *Advanced Materials*, *20*(7), 1263–1269.
Swetha, M., Sahithi, K., Moorthi, A., Srinivasan, N., Ramasamy, K., & Selvamurugan, N. (2010). Biocomposites containing natural polymers and hydroxyapatite for bone tissue engineering. *International Journal of Biological Macromolecules*, *47*(1), 1–4.
Wei, G., & Ma, P. X. (2004). Structure and properties of nano-hydroxyapatite/polymer composite scaffolds for bone tissue engineering. *Biomaterials*, *25*(19), 4749–4757.
Yan, L., Chen, J., & Bangal, P. R. (2007). Dissolving cellulose in a NaOH/thiourea aqueous solution: A topochemical investigation. *Macromolecular Bioscience*, *7*(9–10), 1139–1148.
Yang, Q., Lue, A., Qi, H., Sun, Y., Zhang, X., & Zhang, L. (2009). Properties and bioapplications of blended cellulose and corn protein films. *Macromolecular Bioscience*, *9*(9), 849–856.
Zhou, Q., Zhang, L., Li, M., Wu, X., & Cheng, G. (2005). Homogeneous hydroxyethylation of cellulose in NaOH/urea aqueous solution. *Polymer Bulletin*, *53*(4), 243–248.